Results

Dsg3$^{-/-}$ mice, but not wild-type mice, produced anti-Dsg3 IgG capable of binding to the native mouse Dsg3 on living keratinocytes.

Initially, we tested various wild-type mice (C57BL/6N, BALB/c, and C3H/HeJ) for their ability to produce anti-Dsg3 IgG upon immunization. However, none of them produced IgG that was able to recognize the native form of mouse Dsg3 (data not shown). We believed this failure was likely due to immunological tolerance against mouse Dsg3, a self-antigen.

Such tolerance should not be acquired in mice that are genetically deficient in Dsg3. When we immunized Dsg3$^{-/-}$ mice with mouse rDsg3, anti-Dsg3 IgG was indeed produced. The ELISA titers against rDsg3 became positive at day 11 in Dsg3$^{-/-}$ mice and their titers continued to increase thereafter (Fig. 1A). These sera were able to bind to the cell surfaces of living cultured mouse keratinocytes (Fig. 1B, panel a), indicating that the anti-Dsg3 IgG produced in Dsg3$^{-/-}$ mice is capable of binding to the native Dsg3 on living keratinocytes. In contrast, although the ELISA titers of Dsg3$^{+/-}$ littermates became positive after repeated immunization, their titers were lower than those of Dsg3$^{-/-}$ mice (day 33, p=0.0016). More importantly, the sera from Dsg3$^{+/-}$ mice failed to bind to the surface of living keratinocytes (Fig. 1B, panel b). In addition, there was no *in vivo* deposition of IgG in the stratified squamous epithelia of the immunized Dsg3$^{+/-}$ mice (data not shown). Therefore, most of the antibodies developed in Dsg3$^{+/-}$ mice may have been raised against minor contaminants of the recombinant protein preparation, tags introduced at the C-terminus of rDsg3 or degraded products.

These findings indicate that Dsg3$^{-/-}$ mice and mice expressing Dsg3 have

a clear difference in their ability to produce anti-Dsg3 IgG that can bind to the native Dsg3.

Stable production of anti-Dsg3 IgG by lymphocytes of immunized Dsg3$^{-/-}$ mice in the recipient Rag-2$^{-/-}$ mice

Despite the production of anti-Dsg3 IgG, no autoimmune reaction is expected in the immunized Dsg3$^{-/-}$ mice because they lack the target antigen. To allow the anti-Dsg3 IgG to be exposed to the antigen, we isolated splenocytes from the immunized Dsg3$^{-/-}$ mice, or from Dsg3$^{+/-}$ mice as controls, and transferred them into Rag-2$^{-/-}$ immunodeficient mice (17) that do express Dsg3. Rag-2$^{-/-}$ mice have no mature T or B cells due to the inability to rearrange T cell receptor or immunoglobulin genes and thus are unable to produce antibodies or reject the transferred splenocytes.

Circulating anti-Dsg3 IgG was detected in the sera of recipient Rag-2$^{-/-}$ mice as early as day 4 after the transfer of Dsg3$^{-/-}$ splenocytes. The level increased rapidly without further boosting by rDsg3, and reached a plateau around day 21 (Fig. 2A). The circulating anti-Dsg3 IgG was detected as long as these mice were assayed, which was over 6 months, indicating that endogenous Dsg3 in the recipient mice stimulated the transferred Dsg3-specific lymphocytes from the immunized Dsg3$^{-/-}$ mice *in vivo*. Furthermore, the ELISPOT assay also detected anti-Dsg3 IgG-producing B cells in the spleen and lymph nodes of the recipient mice 4 months after the adoptive transfer (Table 1), confirming the persistent ongoing antibody production. No significant reactivity against Dsg1, another desmosomal cadherin targeted in pemphigus foliaceus, was observed in these recipient mice during this period (Fig. 2A). In marked contrast, no circulating anti-Dsg3 IgG was detected in Rag-2$^{-/-}$ mice given Dsg3$^{+/-}$ splenocytes (Fig. 2A), although the numbers of

$CD4^+$ T cells and $CD19^+$ B cells from $Dsg3^{+/-}$ mice were comparable with those from $Dsg3^{-/-}$ mice in the recipient mice (data not shown).

Rag-$2^{-/-}$ mice with immunized $Dsg3^{-/-}$ splenocytes develop PV phenotypes.

The first symptom we noticed in the recipient Rag-$2^{-/-}$ mice that received immunized $Dsg3^{-/-}$ splenocytes was weight loss that began between day 7 and 14 after the adoptive transfer (Fig. 2B, and 3A, Table 2). In the following days, these mice continued to lose weight and some of them died. The mice that survived started to gain weight again about day 35. Some of these recipient Rag-$2^{-/-}$ mice developed crusted erosions on the skin around the snout (Fig. 3B), an area that is normally traumatized by scratching.

In Rag-$2^{-/-}$ mice that received immunized $Dsg3^{-/-}$ splenocytes, *in vivo* IgG deposition was found on keratinocyte cell surfaces in stratified squamous epithelium, including the skin (Fig. 3C, around the snout), and oral (Fig. 3D, hard palate) and esophageal mucous membranes, just as seen in patients with PV (Fig. 3F). In the epidermis where there were multiple layers of keratinocytes, IgG deposition was limited to the lower layers, while in the oral and esophageal epithelium IgG was found throughout the layers of living epithelium. In these mice, no IgG deposition was found in other tissues, including heart, lung, liver, kidney, stomach, and small and large intestines (data not shown). These IgG binding sites correspond to the known tissue distribution of Dsg3 (5, 20, 21).

Histological examination of the recipient mice revealed an intraepithelial loss of cell-cell adhesion just above the basal layers, i.e. suprabasilar acantholysis, in the buccal mucosa, hard palate (Fig. 3G), oropharyngeal areas, and the upper part of the esophagus (Fig. 3H). These are typical histological

findings in PV patients (Fig. 3J). These oral erosions likely inhibited food intake, resulting in the weight loss. No significant infiltration of inflammatory cells was observed in the early stages of developing blisters (Fig. 3G, H). In contrast, no phenotypic or pathological changes were observed in Rag-2$^{-/-}$ mice that received immunized Dsg3$^{+/-}$ splenocytes (Fig. 3E, I). There was no apparent sign of graft-versus-host disease in the skin or intestines in any of these mice with Dsg3$^{-/-}$ or Dsg3$^{+/-}$ splenocytes (data not shown).

All 18 recipient mice with Dsg3$^{-/-}$ splenocytes showed positive *in vivo* IgG deposition on keratinocyte cell surfaces, although three of them did not show apparent weight loss or histologic acantholysis (Table 2). The IgG titers in these three mice were significantly lower than those in the other 15 mice (peak index values, 2.4+/-0.9x10^3 vs. 0.7+/-0.4x10^3, $p<0.01$). When mice with lower titers were boosted with rDsg3, the titers rose and the mice developed the PV phenotypes (data not shown). Therefore, the appearance of the PV phenotypes might generally be correlated with the antibody titer.

These results indicate that the Rag-2$^{-/-}$ mice given immunized Dsg3$^{-/-}$ splenocytes developed clinical, histologic and immunopathologic phenotypes similar to those of PV patients.

Rag-2$^{-/-}$ mice with immunized Dsg3$^{-/-}$ splenocytes develop alopecia.

Around 15-25 days after the adoptive transfer, we also observed patchy hair loss in the Rag-2$^{-/-}$ mice that received immunized Dsg3$^{-/-}$ splenocytes (Fig. 2A, see arrows, Fig. 4A, B), but not in the Rag-2$^{-/-}$ mice that received Dsg3$^{+/-}$ splenocytes. Typically, the bald areas started as a small spot and gradually enlarged peripherally over the next two to three weeks. In some mice, new hair grew in the bald areas in a patchy pattern (Fig. 4C), while in others, the bald areas remained in the same spot for more than one month. Some mice had

diffuse hair loss with no discrete bald areas. This hair loss phenotype also persisted for over 6 months. Skin biopsy showed intense IgG deposition on the cell surface of keratinocytes surrounding the telogen hair club (Fig. 4D). Cleft formation was observed between the cells surrounding the telogen club and the basal layer of the outer root sheath epithelium (Fig. 4E). The bald skin contained empty, dilated telogen hair follicles, consistent with the loss of the telogen hair (Fig. 4F). These clinical and histological findings of telogen hair loss are virtually identical to those observed in Dsg3$^{-/-}$ mice, as are the findings of erosions on the oral mucous membrane and the skin (13, 22), confirming the specificity and pathogenicity of the anti-Dsg3 IgG produced in these mice.

Discussion

In this study, we adopted a unique approach to develop an active disease mouse model of pemphigus, by assuming that self-tolerance against Dsg3 is lost in $Dsg3^{-/-}$ mice. Immunization with mouse rDsg3 was indeed successful in generating anti-Dsg3 IgG capable of binding native mouse Dsg3 on living keratinocytes in $Dsg3^{-/-}$ mice, but not in $Dsg3^{+/-}$ littermates. When splenocytes containing activated lymphocytes specific for mouse Dsg3 were adoptively transferred to $Rag\text{-}2^{-/-}$ immunodeficient mice that expressed Dsg3, the Dsg3-specific lymphocytes encountered the endogenous Dsg3, resulting in stable production of anti-Dsg3 IgG antibody for over 6 months. The adoptive transfer of purified T cells and B cells from $Dsg3^{-/-}$ mice was sufficient to produce such anti-Dsg3 IgG (Amagai et al., unpublished data), excluding the possible involvement of other types of cells, including antigen-presenting cells from $Dsg3^{-/-}$ mice, in this antibody production. In contrast, the endogenous Dsg3 did not stimulate lymphocytes from immunized $Dsg3^{+/-}$ mice and no anti-Dsg3 IgG was produced in the recipient mice. The persistent ongoing production of IgG against Dsg3 in the $Rag\text{-}2^{-/-}$ mice given $Dsg3^{-/-}$ splenocytes up to 4 months after the transfer was confirmed by the ELISPOT assay. Furthermore, the anti-Dsg3 IgG was pathogenic and the recipient $Rag\text{-}2^{-/-}$ mice developed symptoms of PV, including erosions in the mucous membranes, which inhibited food intake with resultant weight loss, and scaly crusted erosions on traumatized skin, which resembles Nikolsky's sign (gentle rubbing of skin of normal appearance induces blisters). Consequently, this new approach has provided us with a novel active disease animal model of PV.

Clinically, PV is divided into a mucosal dominant type and a mucocutaneous type. In mucosal-dominant PV oral erosions predominate, with limited skin involvement. In mucocutaneous PV, there are extensive skin

lesions in addition to oral involvement. Recently, it was demonstrated that this clinical difference is defined by the anti-Dsg autoantibody profile (14, 23-25). Patients with mucosal dominant PV have anti-Dsg3 IgG alone, while patients with mucocutaneous PV have anti-Dsg1 IgG in addition to anti-Dsg3 IgG. In the epidermis, Dsg1 is co-expressed where Dsg3 is expressed. Therefore, anti-Dsg3 IgG alone is not able to cause skin blisters efficiently. On the other hand, in the mucous membrane Dsg3 is the dominant Dsg isotype and anti-Dsg3 IgG alone is sufficient to cause oral erosions. In our model, Dsg3$^{-/-}$ mice did not develop anti-Dsg1 IgG that was able to access the native Dsg1, because there was no *in vivo* IgG deposition in the immunized Dsg3$^{-/-}$ mice that do express Dsg1, even after repeated immunization (data not shown). Furthermore, the Rag-2$^{-/-}$ recipient mice with Dsg3$^{-/-}$ splenocytes did not develop any apparent anti-Dsg1 IgG with time (Fig. 2A). This finding is consistent with our observation that the phenotypes of recipient mice were virtually identical to those of Dsg3$^{-/-}$ mice. Collectively, the PV model generated in this study represents the mucosal dominant type of PV, because the IgG produced was essentially specific for Dsg3.

Among the PV phenotypes that the recipient mice developed, *in vivo* IgG deposition on keratinocyte cell surfaces was found in all 18 mice with Dsg3$^{-/-}$ splenocytes (Table 2). This *in vivo* antibody binding to the target antigen is the first and essential step leading to the development of the PV phenotypes. Acantholysis in the oral mucosa with resultant weight loss was observed in 15 out of the 18 mice, and the mice without this phenotype had lower titers of anti-Dsg3 IgG. Telogen hair loss was observed less frequently than acantholysis or weight loss (Table 2). In mice, hair follicles in any particular area cycle in a synchronous fashion and enter the same stage at approximately the same time (26). This tendency becomes less evident as mice

age. In addition, for a certain period mice have a normal coat, because hair regrows when the hair cycle enters the anagen stage (22). Therefore, the hair loss phenotype might have been missed because some mice died or were sacrificed before the hair loss became apparent.

Previously, an *in vivo* experimental model of PV was developed by reconstituting severe combined immunodeficiency (SCID) mice with PBMC from patients with PV (27). In this model, lymphocytes from the patients produced a low titer of circulating anti-human Dsg3 IgG, but the spontaneous intra-epidermal blisters associated with human IgG deposits were seen only rarely in mouse skin. After grafting human skin on the SCID mice, PV-like blisters were observed in the grafted skin, although it remains to be determined whether inflammatory reactions due to possible histoincompatibility of human PBMC and skin contributed to the blister development in that model. Therefore, the mouse model developed in the current study is the first solid active disease model of PV.

A major hurdle in developing animal models of autoimmune diseases has been overcoming self-tolerance. To create our model of disease, we circumvented this problem by immunizing autoantigen knockout mice with the autoantigen, then transferring their splenocytes to Rag-2$^{-/-}$ mice that expressed the autoantigen. Although this model does not address the usual triggers of autoimmune diseases, it does provide a means to investigate the roles of T and B lymphocytes in perpetuating autoantibody production in the autoimmune response. In addition, this active animal model should be beneficial for evaluating various therapeutic strategies that could modulate the autoimmune response. Finally, since it is very easy to evaluate disease activity in this model through weight loss and hair loss, it can be used for efficient screening of various therapeutic interventions.

Our approach is widely applicable to various antibody-mediated and T cell-mediated autoimmune diseases unless the relevant autoantigen knockout mice are embryonic lethal or show gross abnormalities in their immune systems. Furthermore, this approach provides another dimension in the use of knockout mice to study the function of target molecules *in vivo*.

Acknowledgments

We thank Dr. John R. Stanley for reviewing the manuscript and insightful discussion and Dr. Tasuku Honjo for valuable discussion. We also thank Drs. John R. Stanley and Leonard D. Shultz for breeding pairs of Dsg3$^{-/-}$ mice, Dr. Jouni Uitto for providing mouse Dsg3 cDNA, and Drs. Norihisa Matsuyoshi, John Stanley, Leena Pulkinen, and Jouni Uitto for providing mouse Dsg1 cDNA. Thanks also go to Dr. Akihiro Umezawa for preparing pathological slides, Ms. Yoshiko Fujii for cell culture and for preparing recombinant baculoproteins, Ms. Minae Suzuki for immunofluorescence staining, and Ms. Ayumi Sakurai for animal care.

This work was supported by Health Sciences Research Grants for Research on Specific Diseases from the Ministry of Health and Welfare (to M. A.), a Grant-in-Aid of Scientific Research (to M.A., S.K., and T.N.), a Grant-in-Aid of International Scientific Research (to T.N.) from the Ministry of Education, Science, Sports and Culture of Japan, Keio Gijuku Academic Development Funds (to M.A.), and a grant from the Japan Society for the Promotion of Science (to S.K., JSPS-RFTF97L00701).

References

1. MacDonald, H.R. 1989. Mechanisms of immunological tolerance. *Science.* 246:982.
2. Goodnow, C.C. 1996. Balancing immunity and tolerance: deletion and tuning lymphocyte repertoires. *Proc Natl Acad Sci USA.* 93:2264-2271.
3. Bach, J.F., Koutouzov, S., and van Endert, P.M. 1998. Are there unique autoantigens triggering autoimmune diseases? *Immunol Rev.* 164:139-155.
4. Stanley, J.R. 1998. Pemphigus. *In* Dermatology in General Medicine. I. M. Freedberg, A. Z. Eisen, K. Wolff, K. F. Austen, L. A. Goldsmith, S. I. Katz, and T. B. Fitzpatrick, editors. McGraw-Hill, New York. 654-666.
5. Amagai, M., Klaus-Kovtun, V., and Stanley, J.R. 1991. Autoantibodies against a novel epithelial cadherin in pemphigus vulgaris, a disease of cell adhesion. *Cell.* 67:869-877.
6. Stanley, J.R. 1993. Cell adhesion molecules as targets of autoantibodies in pemphigus and pemphigoid, bullous diseases due to defective epidermal cell adhesion. *Adv Immunol.* 53:291-325.
7. Amagai, M. 1996. Pemphigus: autoimmunity to epidermal cell adhesion molecules. *Adv Dermatol.* 11:319-352.
8. Schiltz, J.R., and Michel, B. 1976. Production of epidermal acantholysis in normal human skin in vitro by the IgG fraction from pemphigus serum. *J Invest Dermatol.* 67:254-260.
9. Hashimoto, K., Shafran, K.M., Webber, P.S., Lazarus, G.S., and Singer, K.H. 1983. Anti-cell surface pemphigus autoantibody stimulates plasminogen activator activity of human epidermal cells. *J Exp Med.*

157:259-272.

10. Anhalt, G.J., Labib, R.S., Voorhees, J.J., Beals, T.F., and Diaz, L.A. 1982. Induction of pemphigus in neonatal mice by passive transfer of IgG from patients with the disease. *N Engl J Med.* 306:1189-1196.
11. Amagai, M., Karpati, S., Prussick, R., Klaus-Kovtun, V., and Stanley, J.R. 1992. Autoantibodies against the amino-terminal cadherin-like binding domain of pemphigus vulgaris antigen are pathogenic. *J Clin Invest.* 90:919-926.
12. Amagai, M., Nishikawa, T., Nousari, H.C., Anhalt, G.J., and Hashimoto, T. 1998. Antibodies against desmoglein 3 (pemphigus vulgaris antigen) are present in sera from patients with paraneoplastic pemphigus and cause acantholysis *in vivo* in neonatal mice. *J Clin Invest.* 102:775-782.
13. Koch, P.J., Mahoney, M.G., Ishikawa, H., Pulkkinen, L., Uitto, J., Shultz, L., Murphy, G.F., Whitaker-Menezes, D., and Stanley, J.R. 1997. Targeted disruption of the pemphigus vulgaris antigen (desmoglein 3) gene in mice causes loss of keratinocyte cell adhesion with a phenotype similar to pemphigus vulgaris. *J Cell Biol.* 137:1091-1102.
14. Ishii, K., Amagai, M., Hall, R.P., Hashimoto, T., Takayanagi, A., Gamou, S., Shimizu, N., and Nishikawa, T. 1997. Characterization of autoantibodies in pemphigus using antigen-specific ELISAs with baculovirus expressed recombinant desmogleins. *J Immunol.* 159:2010-2017.
15. Amagai, M., Hashimoto, T., Shimizu, N., and Nishikawa, T. 1994. Absorption of pathogenic autoantibodies by the extracellular domain of pemphigus vulgaris antigen (Dsg3) produced by baculovirus. *J Clin Invest.* 94:59-67.
16. Amagai, M., Hashimoto, T., Green, K.J., Shimizu, N., and Nishikawa, T.

1995. Antigen-specific immunoadsorption of pathogenic autoantibodies in pemphigus foliaceus. *J Invest Dermatol.* 104:895-901.

17. Schulz, R.J., Parkes, A., Mizoguchi, E., Bhan, A.K., and Koyasu, S. 1996. Development of $CD4^{-}CD8^{-}$ $\alpha\beta TCR^{+}NK1.1^{+}$ T lymphocytes: thymic selection by self antigen. *J Immunol.* 157:4379-4389.
18. Amagai, M., Komai, A., Hashimoto, T., Shirakata, Y., Hashimoto, K., Yamada, T., Kitajima, Y., Ohya, K., Iwanami, H., and Nishikawa, T. 1999. Usefulness of enzyme-linked immunosorbent assay (ELISA) using recombinant desmogleins 1 and 3 for serodiagnosis of pemphigus. *Br J Dermatol.* 140:351-357.
19. Yuspa, S.H., Hawley-Nelson, P., Koehler, B., and Stanley, J.R. 1980. A survey of transformation markers in differentiating epidermal cell lines in culture. *Cancer Res.* 40:4694-4703.
20. Schafer, S., Koch, P.J., and Franke, W.W. 1994. Identification of the ubiquitous human desmoglein, Dsg2, and the expression catalogue of the desmoglein subfamily of desmosomal cadherins. *Exp Cell Res.* 211:391-9.
21. Amagai, M., Koch, P.J., Nishikawa, T., and Stanley, J.R. 1996. Pemphigus vulgaris antigen (Desmoglein 3) is localized in the lower epidermis, the site of blister formation in patients. *J Invest Dermatol.* 106:351-355.
22. Koch, P.J., Mahoney, M.G., Cotsarelis, G., Rothenberger, K., Lavker, R.M., and Stanley, J.R. 1998. Desmoglein 3 anchors telogen hair in the follicle. *J Cell Sci.* 111:2529-2537.
23. Ding, X., Aoki, V., Mascaro, J.M., Lopez-Swiderski, A., Diaz, L.A., and Fairley, J.A. 1997. Mucosal and mucocutaneous (generalized) pemphigus vulgaris show distinct autoantibody profiles. *J Invest Dermatol.* 109:592-596.

24. Amagai, M., Tsunoda, K., Zillikens, D., Nagai, T., and Nishikawa, T. 1999. The clinical phenotype of pemphigus is defined by the anti-desmoglein autoantibody profile. *J Am Acad Dermatol.* 40:167-170.

25. Mahoney, M.G., Wang, Z., Rothenberger, K.L., Koch, P.J., Amagai, M., and Stanley, J.R. 1999. Explanation for the clinical and microscopic localization of lesions in pemphigus foliaceus and vulgaris. *J Clin Invest.* 103:461-468.

26. Dry, F.W. 1926. The coat of the mouse (*Mus musculus*). *J Genet.* 16:287-340.

27. Juhasz, I., Lazarus, G.S., Murphy, G.F., Shih, I.M., and Herlyn, M. 1993. Development of pemphigus vulgaris-like lesions in severe combined immunodeficiency disease mice reconstituted with lymphocytes from patients. *J Clin Invest.* 92:2401-7.

Figure Legends

Figure 1. Anti-Dsg3 IgG antibodies that can bind the native Dsg3 *in vivo* are produced in $Dsg3^{-/-}$ mice, but not in $Dsg3^{+/-}$ mice. (A) $Dsg3^{-/-}$ mice and their $Dsg3^{+/-}$ littermates were immunized with mouse rDsg3 and the ELISA titers against rDsg3 were measured over time. Mice were primed by intraperitoneal injection of purified mouse rDsg3 in complete Freund's adjuvant on day 0 (arrow), then boosted with mouse rDsg3 in incomplete Freund's adjuvant (solid triangle) then without adjuvant (open triangle). (B) A mouse keratinocyte cell line, PAM212, was incubated with mouse serum samples in culture media in a CO_2 incubator for 30 min. After washing and fixation with methanol, bound mouse IgG was visualized with FITC-conjugated goat anti-mouse IgG antibodies. Sera from immunized $Dsg3^{-/-}$ mice (a), but not from their $Dsg3^{+/-}$ littermates (b), stained the cell-cell contact sites of cultured keratinocytes. The bar indicates 50 μm.

Figure 2. Stable production of anti-Dsg3 IgG in mice given immunized $Dsg3^{-/-}$ splenocytes. Splenocytes were isolated from immunized $Dsg3^{-/-}$ or $Dsg3^{+/-}$ mice and transferred to $Rag\text{-}2^{-/-}$ mice by intravenous injection into the tail vein. (A) Circulating anti-Dsg3 IgG was detected in the recipient mice that received $Dsg3^{-/-}$ splenocytes (open symbols, solid line), but not in the recipients of $Dsg3^{+/-}$ splenocytes (solid symbols). The antibody production persisted for over 6 months. There was no apparent reactivity against Dsg1 (dashed line). Arrows indicate the day when the hair loss phenotype became apparent. (B) The weight changes of the recipient $Rag\text{-}2^{-/-}$ mice was plotted against time. † indicate the death of a mouse.

Figure 3. Rag-2$^{-/-}$ recipient mice transferred with immunized Dsg3$^{-/-}$ splenocytes develop PV phenotypes. (A) From 25-35 days after the adoptive transfer, recipient mice given Dsg3$^{-/-}$ splenocytes (bottom) were significantly smaller than those given Dsg3$^{+/-}$ splenocytes (top). (B) Some recipient mice with Dsg3$^{-/-}$ splenocytes developed crusted erosions around the snout and cheeks, where mice normally scratch. (C-J) Histological and immunopathological examination of Rag-2$^{-/-}$ recipient mice and patients with PV. *In vivo* IgG deposition on keratinocyte cell surfaces was observed in the skin (C, around the snout) and mucous membranes (D, hard palate) of the Rag-2$^{-/-}$ mice given Dsg3$^{-/-}$ splenocytes, just as found in patients with PV (F, esophagus, biopsy specimen). In contrast, there was no *in vivo* IgG deposition in the mice given Dsg3$^{+/-}$ splenocytes (E, hard palate). The mice that received Dsg3$^{-/-}$ splenocytes developed intraepithelial blisters just above the basal layers in mucosal epithelium (G, hard palate; H, upper esophagus), which is a typical histological finding in PV patients (J, skin). There was no apparent sign of acantholysis in the mice with Dsg3$^{+/-}$ splenocytes(I, upper esophagus). Bars indicate 50 μm.

Figure 4. Hair loss phenotype of Rag-2$^{-/-}$ mice given immunized Dsg3$^{-/-}$ splenocytes. (A, B) The Rag-2$^{-/-}$ mice given Dsg3$^{-/-}$ splenocytes showed patchy hair loss, which first became apparent around day 15 - 25. (C) New hair growing in a bald area in a patchy pattern (arrows). (D) Intense *in vivo* IgG deposition was noticed on the cell surface of keratinocytes surrounding the telogen hair club. (E, F) Cleft formation between the cells surrounding the telogen club and the basal layer of the

outer root sheath epithelium (E, arrows) and empty, dilated telogen hair follicles (F, arrows). Bars indicate 100 μm.

Table 1. Detection of anti-Dsg3 IgG-producing B cells by ELISPOT assays in Rag-2$^{-/-}$ mice transferred with immunized Dsg3$^{-/-}$ splenocytes.

Mouse	Transfer[A]	Day[B]	Spleen	Lymph node	Bone Marrow	PBMC
RAG#466	-	-	0.0±0.0[C]	0.0±0.0	0.0±0.0	0.0±0.0
RAG#514	+	22	86.5±29.9	13.5±13.6	0.0±0.0	3.8±5.4
RAG#212	+	33	102.1±14.7	47.8±8.8	0.0±0.0	0.0±0.0
RAG#134	+	117	20.8±5.9	16.5±5.9	2.1±2.9	0.0±0.0
RAG#135	+	117	31.3±8.8	27.1±2.9	0.0±0.0	0.0±0.0

[A] Rag-2$^{-/-}$ mice which were transferred with (+) or without (-) splenocytes of immunized Dsg3$^{-/-}$ mice.

[B] Day of sacrifice after the transfer.

[C] Number of Anti-Dsg3 IgG-producing B cells is shown per 10^5 mononuclear cells.

Table 2. Summary of PV phenotypes observed in Rag-2$^{-/-}$ recipient mice.

Rag2-/- mice with	Number tested	Positive ELISA[B]	Living Cell Staining[C]	Positive DIF[D]	Acantholysis in Histology[E]	Weight Loss Phenotype[F]	Crusted Erosive Lesions	Hair Loss Phenotype
Dsg3-/- splenocytes	18[A]	18	18	18	15	15	6	13
Dsg3+/- splenocytes	10	0	0	0	0	0	0	0

[A] Number of mice with positive finding for each category was listed.

[B] Circulating IgG was tested with ELISA against mouse rDsg3.

[C] Circulating IgG was tested with living keratinocyte (PAM212) staining.

[D] *In vivo* IgG deposition on keratinocyte cell surfaces was determined by direct immunofluorescence staining of oropharyngeal mucous membranes.

[E] Intraepithelial blister formation, i.e. suprabasilar acantholysis, was looked for by histology in the oropharyngeal areas.

[F] Weight loss greater than 2 g within a week was considered significant.

A

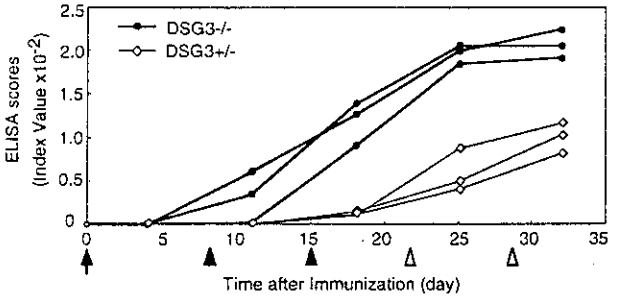
DSG3-/-
DSG3+/-
ELISA scores
(Index Value x10-2)
2.5
2.0
1.5
1.0
0.5
0
0
5
10
15
20
25
30
35
Time after Immunization (day)

B

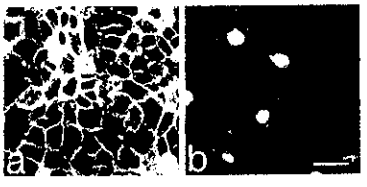
a
b

Fig 1